*Journal of Marine Research, 54,* 541–564, 1996

# Water-property distributions along an eastern Pacific hydrographic section at 135W

**by Mizuki Tsuchiya[1] and Lynne D. Talley[1]**

ABSTRACT

As part of the World Ocean Circulation Experiment, full-depth CTD/hydrographic measurements with high horizontal and vertical resolutions were made in June–August 1991 along a line extending from 34N to 33S at a nominal longitude of 135W with an additional short leg that connects it to the California coast roughly along 34N. The line spans the major part of the subtropical and intertropical circulation regime of the eastern North and South Pacific. The primary purpose of this paper is to present vertical sections of various properties from CTD and discrete water-sample measurements along this line and to give an overview of some important features as a basis for more comprehensive basin-scale studies. These features include: the frontal structures found in the surface-layer salinity field in the North Pacific; relatively high-salinity water that dominates the subpycnocline layer between the equator and 17N; troughs of the subpycnocline isopycnals for 26.8–27.5 $\sigma_\theta$ found at 12N and 12.5S; a permanent thermostad at 9–10°C observed between 4.5N and 15N; the pycnostad of the Subantarctic Mode Water centered at 27.0–27.05 $\sigma_\theta$ and developed south of 22S; two types of the Antarctic Intermediate Water representing the subtropical and equatorial circulation regimes; a thick tongue of high silica centered at 3000 m (45.8 $\sigma_4$) and extending southward across the entire section; deep (2000–3000 m) westward flows at 5–8N and 10–15S separated by an eastward flow at 1–2S; and dense, cold, oxygen-rich, nutrient-poor bottom waters, which are associated with fracture zones and believed to represent the pathways of eastward flows into the Northeast Pacific Basin of the bottom waters separated from the northward-flowing western boundary undercurrent. This work once again demonstrates the usefulness of long lines of high-quality, high-resolution hydrographic stations such as the one described herein in advancing the understanding of the large-scale ocean circulation.

## 1. Introduction

Long full-depth CTD/hydrographic sections with closely spaced stations have been most useful in describing the large-scale ocean circulation and water-characteristic distribution. Such a section was occupied in 1991 in the eastern Pacific as part of the World Ocean Circulation Experiment (WOCE) Hydrographic Program (WHP). The section extends from the California coast approximately zonally to 34.5N, 135W and then turns southward to continue across the equator as far as 33S along a nominal longitude of 135W (Fig. 1). The meridional portion of this section

1. Scripps Institution of Oceanography, University of California, San Diego, La Jolla, CA, 92093-0230, U.S.A.

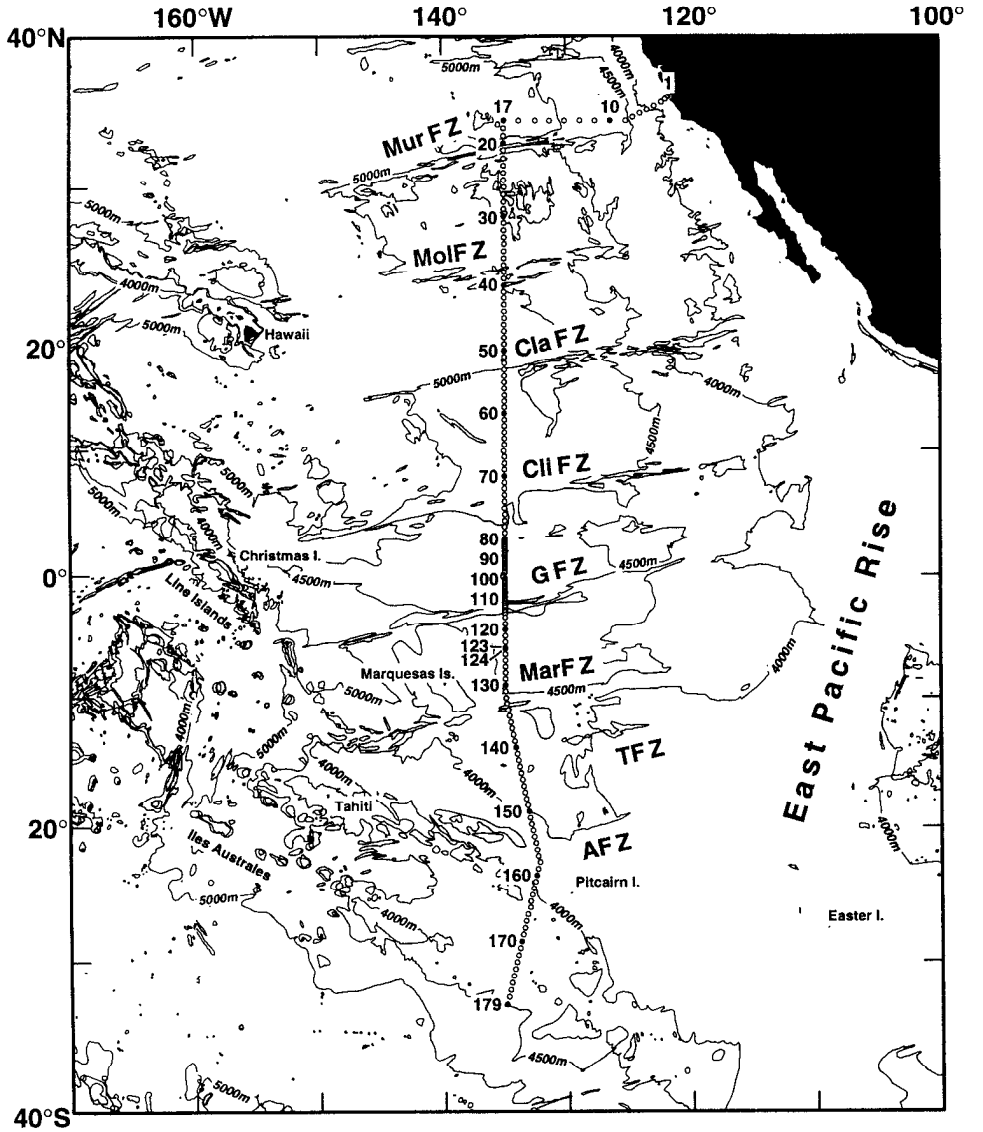


Figure 1. Positions of the stations occupied by R/V *Thomas Washington* on Tunes Legs 1–2, June–August 1991 and used for the vertical sections illustrated in Figures 2–8. The first station of Leg 2 (Sta. 124) was occupied at the same location (6S, 135W) as the last station of Leg 1 (Sta. 123) but 14 days later. The 4000, 4500, and 5000 m isobaths are included. The abbreviations for the fracture zones (FZ) indicated on the map are, from the north, Mur = Murray, Mol = Molokai, Cla = Clarion, Cli = Clipperton, G = Galapagos, Mar = Marquesas, T = Tuamotu, and A = Austral.

**Figures 2 through 8 follow**

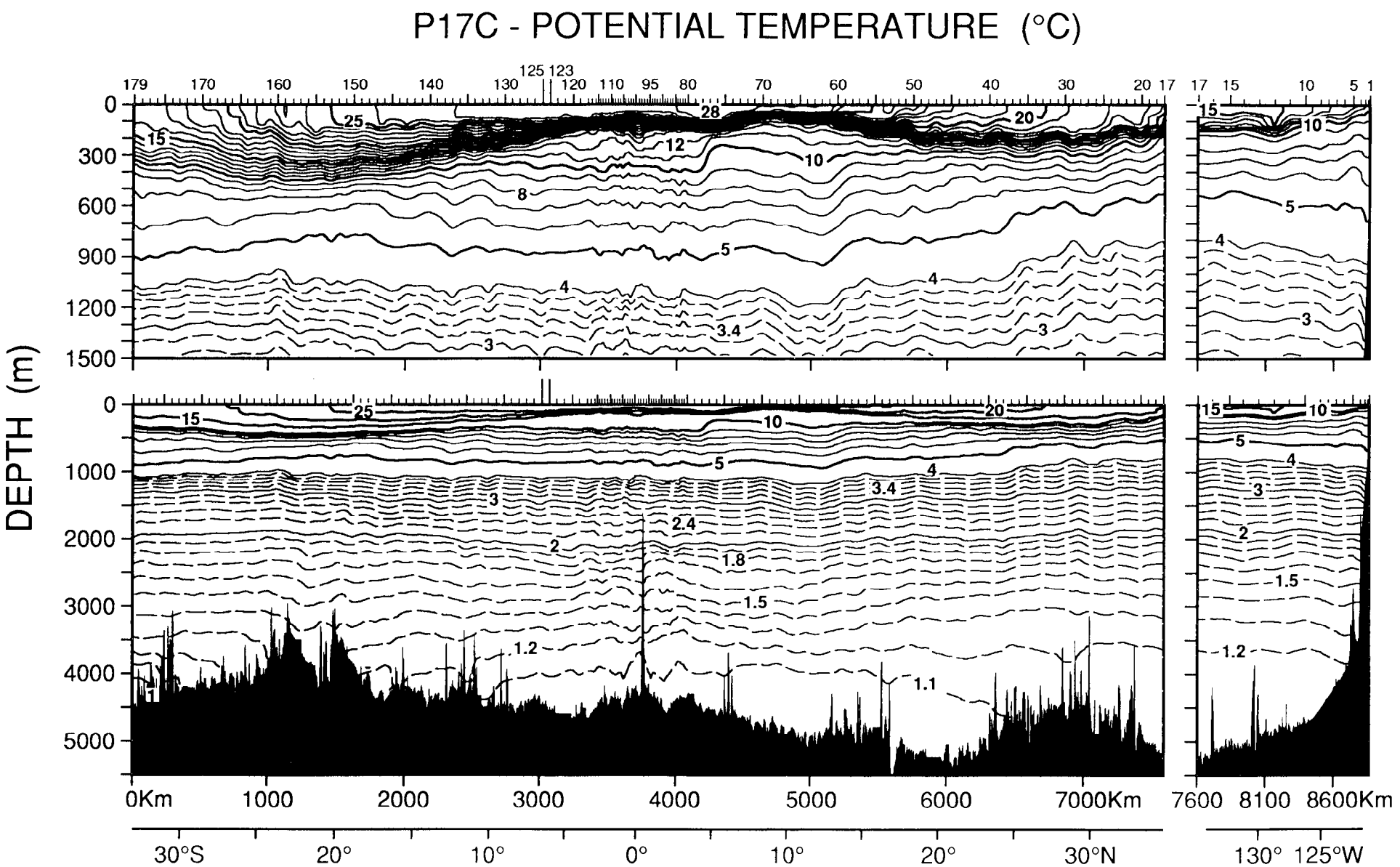


Figure 2. Potential temperature (°C), based on CTD data, along the section shown in Figure 1. The vertical exaggeration is 1250 in the upper panel and 500 in the lower panel.

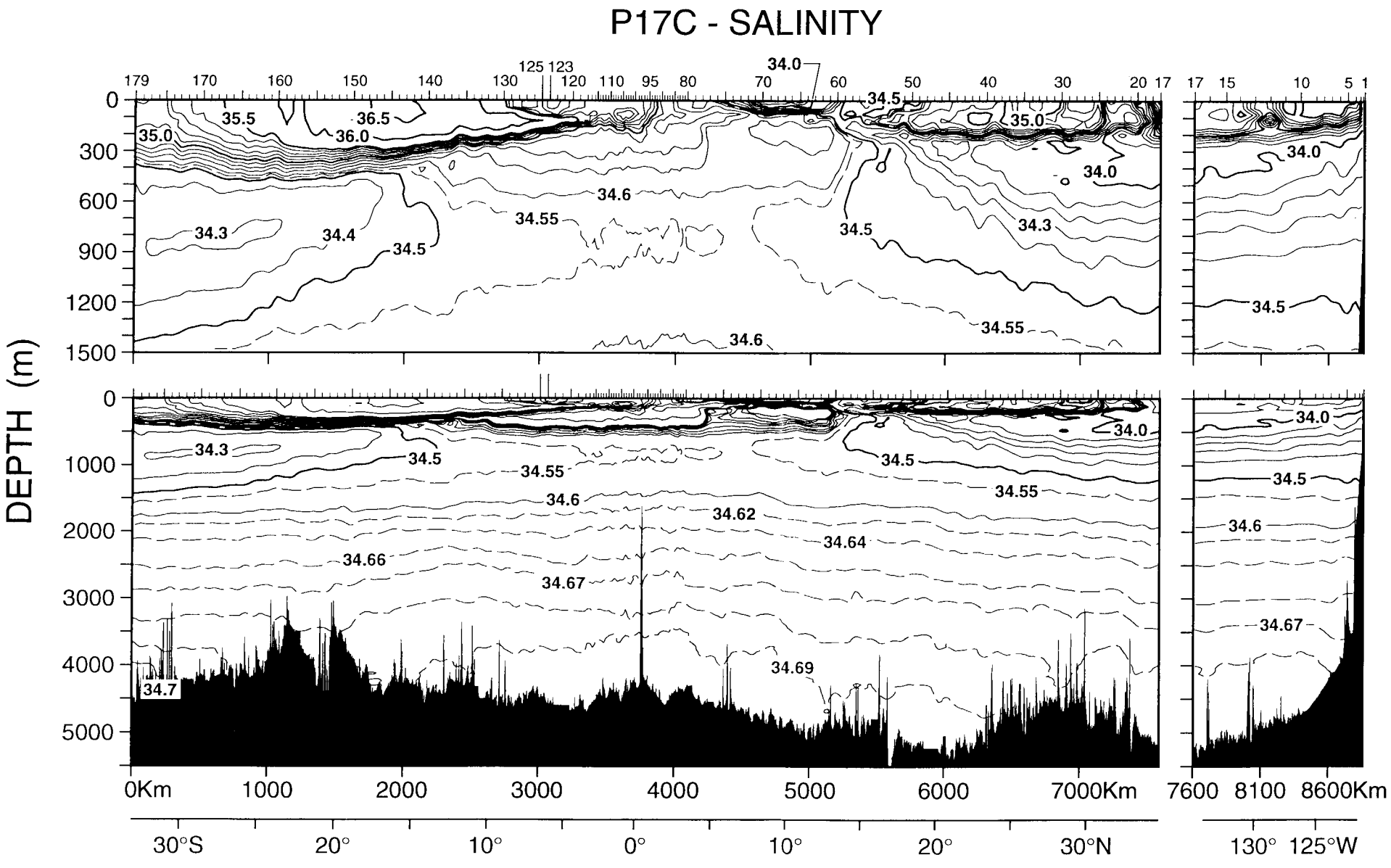


Figure 3. Salinity, based on CTD data, along the section shown in Figure 1.

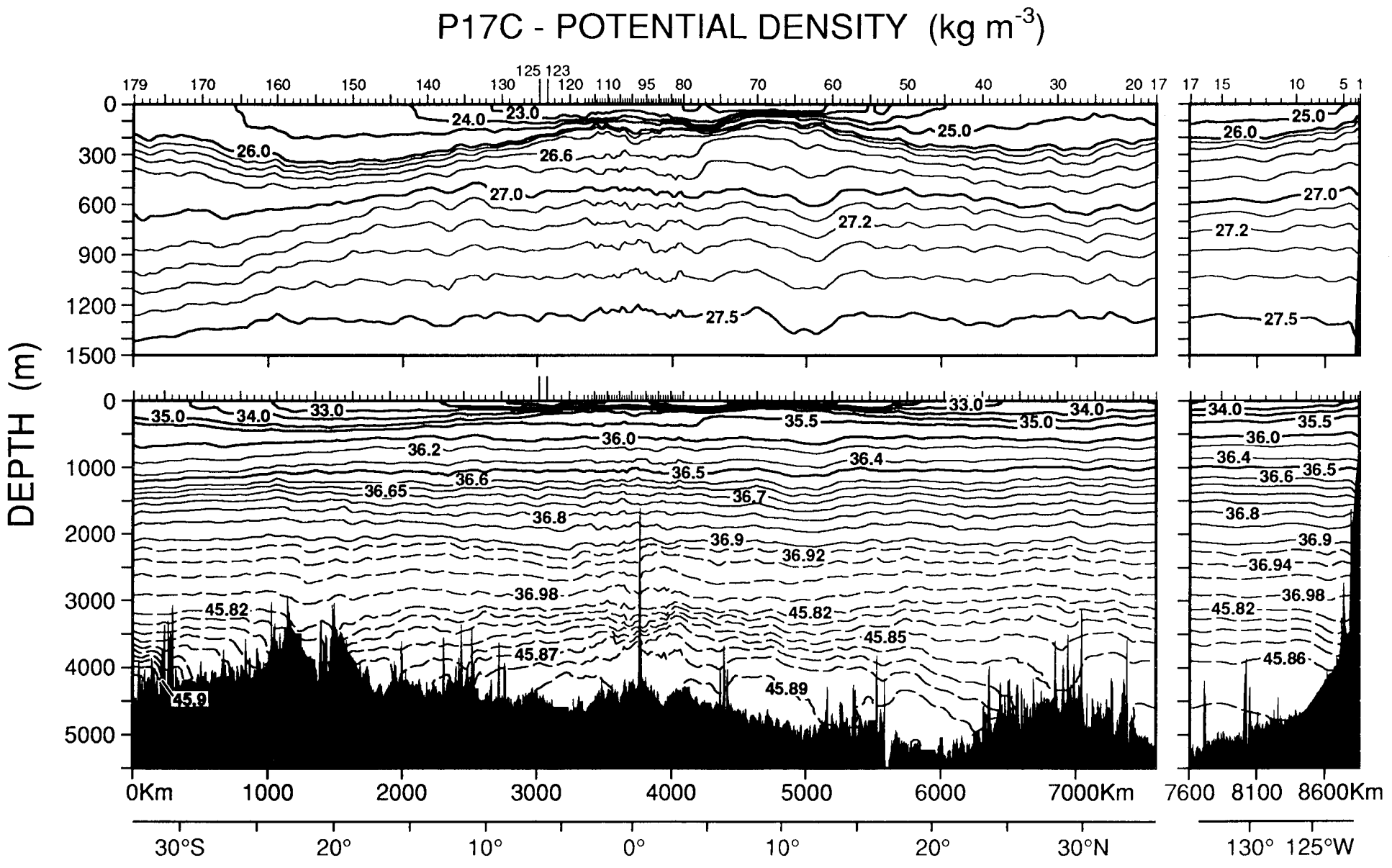


Figure 4. Potential density (kg m $^{-3}$), based on CTD data, along the section shown in Figure 1. The upper panel shows $\sigma_\theta$, while the lower panel shows $\sigma_2$ for 0–3000 m and $\sigma_4$ for depths greater than 3000 m.

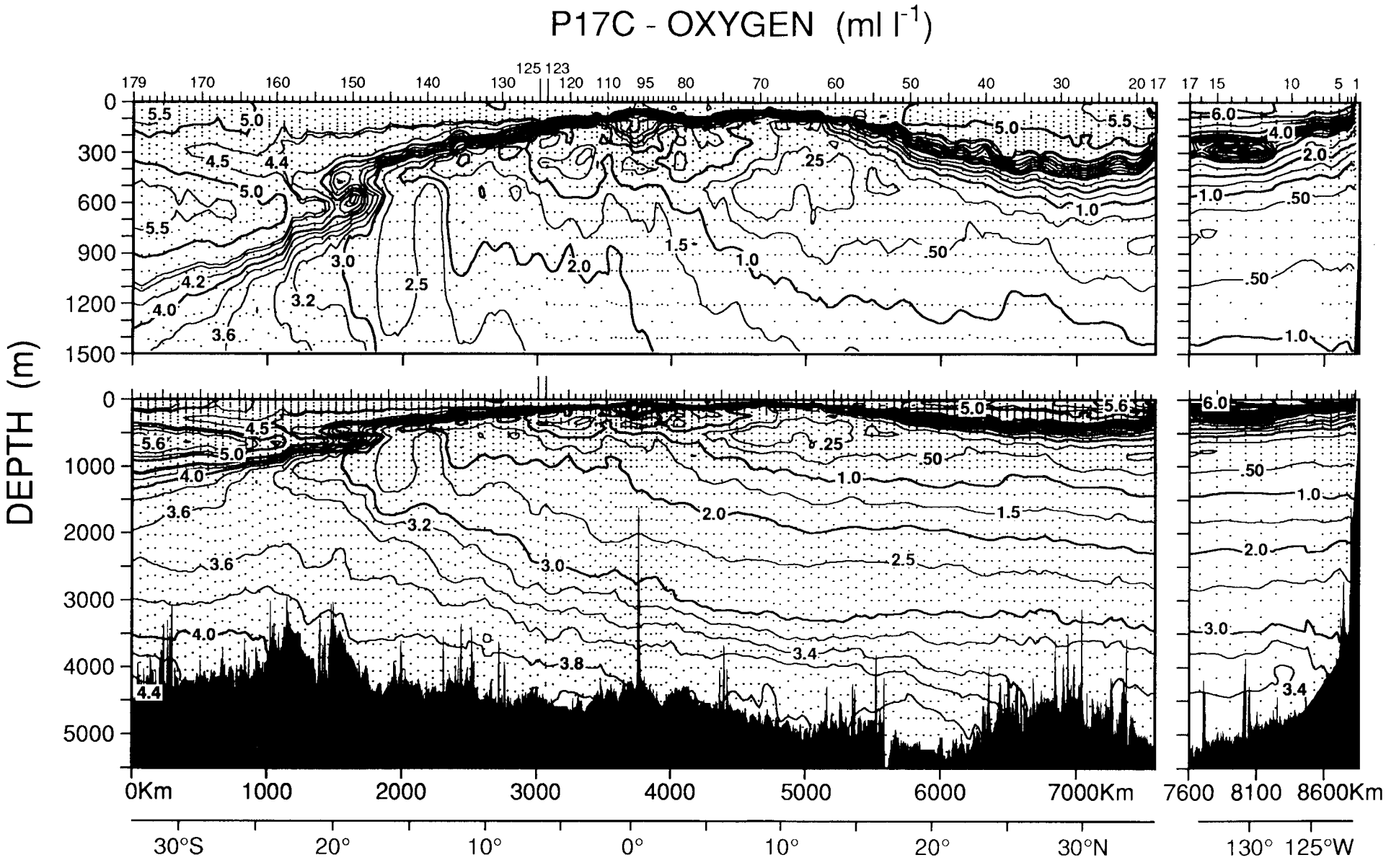


Figure 5. Oxygen (ml $l^{-1}$), based on bottle data, along the section shown in Figure 1.

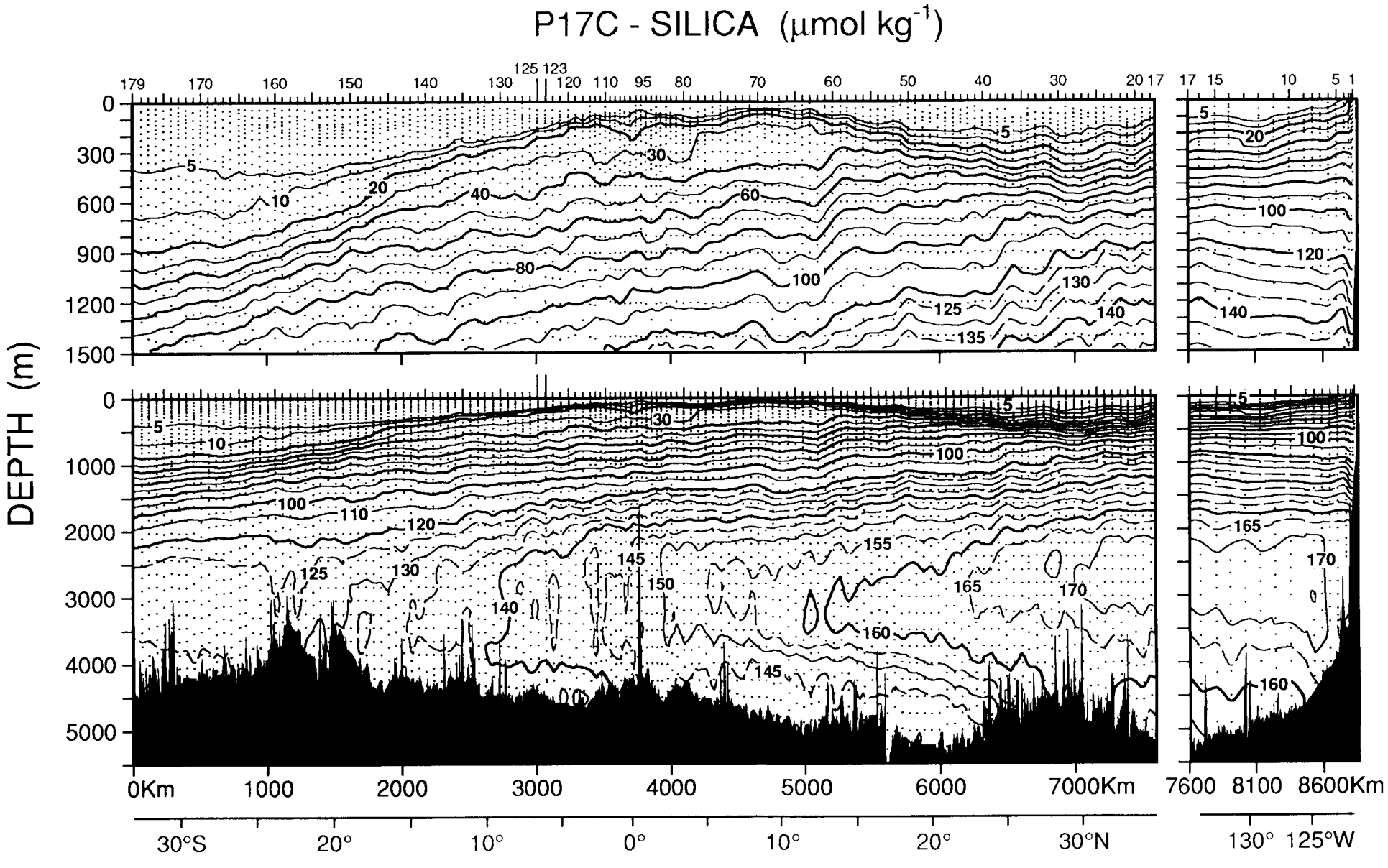


Figure 6. Silica (µmol kg $^{-1}$), based on bottle data, along the section shown in Figure 1.

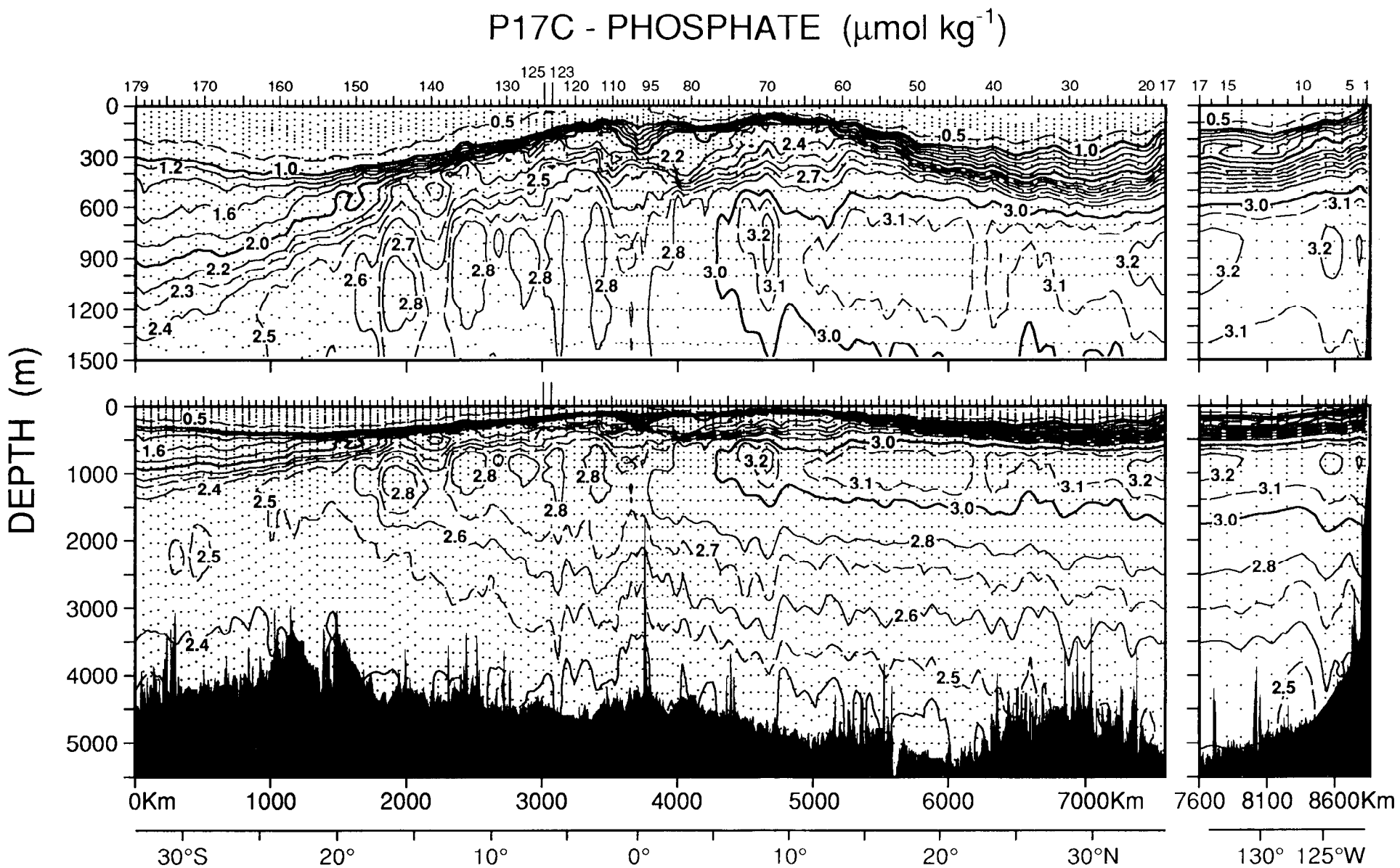


Figure 7. Phosphate (µmol kg $^{-1}$), based on bottle data, along the section shown in Figure 1.

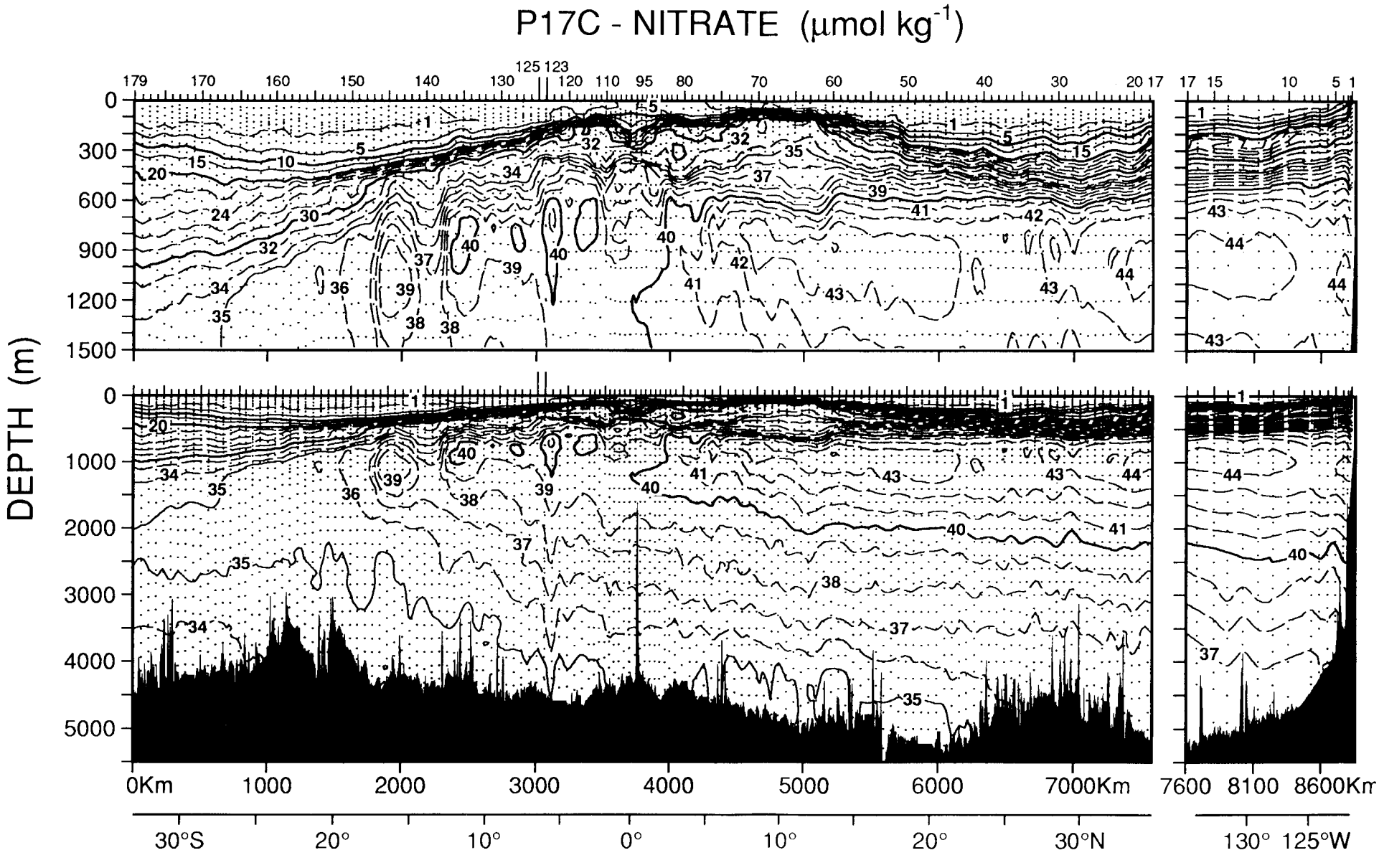


Figure 8. Nitrate (µmol kg $^{-1}$), based on bottle data, along the section shown in Figure 1.

and three other subsequently occupied sections make up a complete meridional section (designated as WOCE P17) extending from Alaska to the south of the Antarctic Circumpolar Current. The primary aim of the WHP is to improve knowledge of the distribution and sources of water masses, and their circulation and transports, with the goal of understanding how the ocean and atmosphere interact on long time scales. Within the framework of the WHP, the present section was made with more specific objectives, which included studies of zonal currents at all depths in the tropics, patterns of cross-equatorial transport, patterns of mid-depth and abyssal flow in the eastern Pacific, and the effect of the major fracture zones on abyssal flow.

While some of these objectives are difficult to achieve without additional spatial information, this paper provides an overview of the major features found in the vertical sections of potential temperature, salinity, potential density ($\sigma_\theta$ and $\sigma_2/\sigma_4$), oxygen, silica, phosphate, and nitrate from this single cruise (Figs. 2–8). It will serve as a fundamental basis for more comprehensive and detailed analyses of combined data from this and other WHP sections covering the entire Pacific Ocean. To facilitate the discussion, some properties on a few specific horizons along 135W are also plotted as functions of latitude and displayed in Figures 9–14.

The field work was carried out on R/V *Thomas Washington* (Expedition Tunes Leg 1 and the first half of Leg 2) in June–August 1991. A total of 179 stations were occupied as shown in Figure 1. Between Sta. 123 (the last station of Leg 1) and Sta. 124 (the first station of Leg 2), which was a reoccupation of Sta. 123, the station work was interrupted for 14 days by a port call at Papeete, Tahiti. Southward from Sta. 132 (10S), where the section intersects a bottom ridge extending from the East Pacific Rise to the Tuamotu Archipelago, stations were displaced slightly to the east and back to cross the ridge at a saddle near 132W. Two stations at and immediately south of the equator were shifted to the west by 19 km to avoid a seamount. Stations were spaced generally at intervals of 56 km, but at closer intervals near the California coast and within 3° of the equator to resolve small-scale features. Along the western half of the 34.5N section, the time constraint due to bad weather necessitated coarser spacing.

On each station a rosette sampler equipped with a CTD was lowered to the bottom. A 36-place 10-liter bottle rosette was used as the principal water-sampling tool. A smaller rosette with 11 bottles was also used on alternate stations between 3N and 3S, where station spacing was 19 km, but water sampling was limited to salt to calibrate the CTD. To assess the quality of the acquired data, they were compared with those from other recent cruises whose tracks crossed ours. The comparisons indicated that, although unexpectedly large differences in some properties were occasionally noted, the overall accuracies of our measurements were within the WOCE specifications (U. S. WOCE Office, 1989).

All density-anomaly values ($\sigma_\theta$, $\sigma_2$, etc.) in this paper are calculated according to

the International Equation of State (EOS80), with the units being kg $m^{-3}$. All salinity values are on the Practical Salinity Scale (PSS78).

## 2. Surface and pycnocline waters

The low-salinity surface water observed at the north end of the 135W section and all along the 34.5N section is of subarctic origin. It is bounded at its base by a halocline centered on the 33.6 isohaline. The halocline is 150–200 m deep and is about 100 m deeper than the thermocline. Near 34N, a sharp horizontal gradient of salinity is indicated by the tightly packed nearly vertical isohalines for 33.2–33.8 in the top 200 m (see also Fig. 9). This gradient represents the subarctic front and forms the southern limit of the subarctic halocline, in which salinity increases downward.

About 1° of latitude south of the subarctic front, another front is indicated by the 34.0–34.2 isohalines. It marks the northern limit of the subtropical halocline, in which salinity decreases downward, and can be interpreted to be the northern subtropical front derscribed by Lynn (1986). It is the eastward continuation of the "34°N front" observed by Roden (1980) in the area north of Hawaii.

At 31N the isohalines for 34.4–34.8, which occupy the major portion of the halocline south of this latitude, rise abruptly to the sea surface. This almost vertical rise of the isohalines forms the subtropical front, in which the 18°C isotherm is embedded. South of the subtropical front, relatively warm, high-salinity water is found above the halocline, which coincides with the thermocline. This high-salinity water ($>35.0$ at its center near 27N) represents the eastern edge of the subtropical water (also called tropical water; e.g., Cannon, 1966) of the North Pacific associated with excess evaporation over precipitation. North of 24N the North Pacific subtropical water shows a salinity maximum at the sea surface, while south of 24N it shows a subsurface salinity maximum extending along $\sigma_\theta \sim 24.5$ as far equatorward as about 13N. This subsurface salinity maximum is roughly coincident with an oxygen maximum.

Low-salinity surface water ($<34.0$) is found at 7–11N near the boundary between the North Equatorial Current and the North Equatorial Countercurrent indicated by the ridge of the pycnocline at ~9N. Rather broad salinity fronts at 12–14N and 5–8N mark its northern and southern boundaries. This low-salinity water is due to high local precipitation, but advection by the North Equatorial Current from the east, where surface salinity is even lower (e.g., Levitus, 1982, Fig. 22), and subsequent lateral mixing may also contribute to it. A previous study by Lynn (1964) showed that the meridional minimum of the surface salinity associated with this low-salinity water in the central and eastern Pacific falls sometimes in the North Equatorial Current and at other times in the Countercurrent. Hires and Montgomery (1972) found that the meridional minimum in the central Pacific lies at 10–11N on the annual average and discussed its annual north-south shift in the North Equatorial Current and

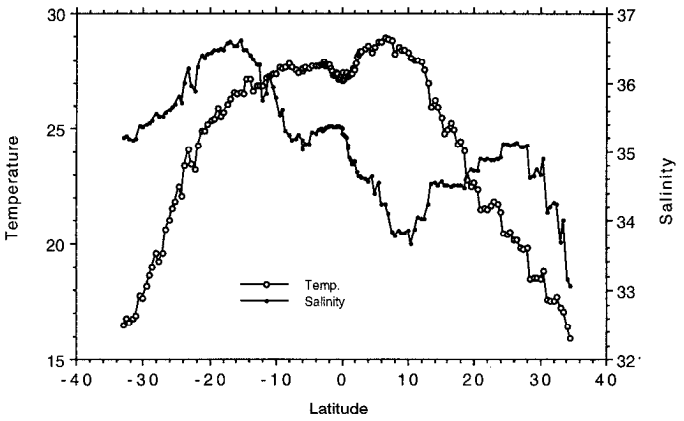


Figure 9. Sea-surface temperature (°C) and salinity, based on bottle measurements, along 135W.

Countercurrent. On the present section the lateral salinity minimum is found near 10N in the North Equatorial Current.

The low-salinity surface water described above is warm with temperatures above 28°C. However, the high temperatures extend southward across the salinity front at 5–8N and the maximum temperature ($\sim$29°C) occurs at 7N within the front. The warm water we observed is nearly 1.5°C warmer than that seen in Robinson's (1976) long-term mean surface-temperature map for June. The well-known equatorial lateral temperature minimum (e.g., Puls, 1895) is obscured by this positive temperature anomaly and is only weakly developed. It is accompanied by a weak temperature maximum near 3S. Both the equatorial minimum and the maximum south of the equator are not resolved by the isotherms at 1°C intervals in Figure 2 but are clearly seen in Figure 9.

Southward from the salinity front at 5–8N, the surface salinity increases to a weak maximum ($>$35.2) located slightly south of the equator. The salinity increase, however, is not uniform with a fairly strong front at 1–2N. The salinity maximum is accompanied by a minimum ($<$35.2) near 6S. This salinity maximum south of the equator was noted by Lynn (1964) and Hires and Montgomery (1972), but they found it in the vicinity of 5S. Farther south near 15S, there is a well-developed lateral salinity maximum ($\sim$36.6), which represents the center of the South Pacific subtropical water associated with excess evaporation. South of the maximum the subtropical water occupies a thick layer (100–250 m) above the halocline with its temperature and salinity decreasing slowly southward. The subtropical water extends also northward underneath the lower-salinity surface water. It forms a high-salinity tongue roughly along the 24.0 $\sigma_\phi$ isopycnal in the pycnocline. There are three separate cores of this high-salinity water, though not all of them are resolved in Figure 3. The first one ($>$35.6), centered at 4S, is associated with the subsurface South Equatorial

Countercurrent (Tsuchiya, 1975), which is indicated by the equatorward dip of the subpycnocline isopycnals for 26.5–26.8 $\sigma_\theta$ and which apparently extends upward into the pycnocline. The second ($>35.4$) is centered at 1S and falls in the Equatorial Undercurrent. The third ($>34.8$) occurs farther north between 3.5N and 7N at somewhat lower density ($\sigma_\theta \sim 23.0$) above the pycnocline. It lies in the domain of eastward flow associated with the surface and subsurface North Equatorial Countercurrents indicated by the equatorward deepening of the pycnocline and the subpycnocline isopycnals for 26.6–27.0 $\sigma_\theta$. As has been pointed out by Montgomery and Stroup (1962), the South Pacific subtropical water extends farther northward to the west of the present section and thus provides these eastward currents with a source of high salinity. Tsuchiya's (1968, Figs. 6 and 7) maps of the salinity distribution in the pycnocline do not indicate a significant contribution from the North Pacific subtropical water.

### 3. Subpycnocline waters

*a. Coastal region.* There is clear evidence of wind-induced coastal upwelling at the eastern end of the 34.5N section. Within a narrow coastal strip about 40 km wide, isopleths of all properties in the upper 200 m rise sharply to the surface exposing cold, oxygen-poor, nutrient-rich subpycnocline waters. The width of the strip is related to the baroclinic radius of deformation (Yoshida, 1955). Below 200 m the slope of isopleths is reversed. This reversal is associated with a poleward undercurrent and is a characteristic feature of coastal upwelling (e.g., Yoshida and Tsuchiya, 1957).

*b. North Pacific subtropical region.* West of ~131W on the 34.5 N section, a vertical salinity minimum is found at $\sigma_\theta = 26.0$ or less near the top of the subarctic halocline. South of the subarctic front, it extends equatorward at the base ($\sim 26.0$ $\sigma_\theta$) of the subtropical halocline. This minimum is distinct from the deeper minimum of the North Pacific Intermediate Water and is identified as the shallow salinity minimum described in detail by Reid (1965, 1973a) and further studied by many other investigators. Recently, Yuan and Talley (1992) examined its southward spreading and evolution along 135W with use of individual station CTD profiles from the present Tunes Leg 1 data set (their Fig. 13). Their study illustrates that the shallow salinity minimum continues southward along $\sigma_\theta \sim 26.0$ above the North Pacific Intermediate Water (26.6–26.7 $\sigma_\theta$) as far as 27N. South of this latitude, the two minima merge to form a single layer of low-salinity water presumably because vertical mixing eliminates the weak maximum that separates the two minima. This low-salinity water, which can no longer be identified either as the North Pacific Intermediate Water or as the shallow salinity minimum, is as thick as 300 m at 26N but becomes thinner and shallower farther south. Its axis lies roughly at 26.2 $\sigma_\theta$. At 17N the subpycnocline high-salinity water described just below (Section 3c) meets

the low-salinity water and intrudes into its lower part (26.6 $\sigma_\theta$) to produce two minima again. The upper minimum occurs at ~26.0 $\sigma_\theta$ and, Yuan and Talley referred to it as the tropical salinity minimum to distinguish it from the shallow minimum north of 27N. The tropical minimum extends equatorward above the subpycnocline high-salinity water at least as far as ~7N. The deeper minimum, which they identified as the Antarctic Intermediate Water, will be discussed in Section 4. (The isohalines drawn in Figure 3 do not resolve every detail of these various salinity extrema, particularly the equatorward extension of the tropical minimum.)

*c. Equatorial region.* Between the equator and 17N, there is a vertical maximum of salinity at 26.5–26.7 $\sigma_\theta$ just below the pycnocline. This high-salinity water forms an isolated core (saltier than 34.7) at 7.5–12N, where the southward rise of isopycnals below the core clearly indicates that it lies in the westward North Equatorial Current. At 5–7N immediately south of the core, the maximum salinity is reduced and the maximum is not revealed by the isohalines in Figure 3. This weakened maximum coincides with the eastward flow of the North Equatorial Countercurrent suggested by the slope of isopycnals below 500 m. South of ~4N the salinity maximum intensifies again and can be recognized by the 34.8 isohaline. A similar subpycnocline salinity maximum directly north of the equator has been observed at 150W by Montgomery and Stroup (1962, Section 1–6), who inferred its source to be to the east of their section. This meridional structure of the subpycnocline high-salinity water in the equatorial North Pacific and its relation with the circulation pattern consisting of bands of alternating zonal flow have been illustrated most clearly in Tsuchiya's (1968) maps of water properties at $\delta_T = 160$ cl $t^{-1}$ ($\sigma_t \sim 26.4$). His salinity map in particular demonstrates that its source is the relatively high-salinity water (>34.8) found from 115W eastward to the coast of Central America. This immediate source water in turn appears to come from the south across the equator.

Near the northern edge of the subpycnocline high-salinity water, the isopycnals for 26.8–27.5 $\sigma_\theta$ form a well-defined trough centered at 12N. The silica, phosphate, and nitrate sections (Figs. 6–8) exhibit similar troughs of subpycnocline isopleths at the same location. With a deep reference pressure, this isopycnal pattern is a signature of a westward geostrophic flow south of 12N and an eastward flow north of 12N. The westward flow is taken to be the southern portion of the North Equatorial Current, and the eastward flow separates it from the westward flow north of ~15N, which apparently represents the northern portion of the North Equatorial Current. The eastward flow and the northern portion of the North Equatorial Current may form a meridionally narrow cyclonic gyre whose zonal scale is not known. There are previous observations in the central and eastern Pacific that suggest a similar trough of the same isopycnals at about the same latitude (e.g., Montgomery, 1954; Craig *et al.,* 1981; Taft and Kovala, 1981; Taft *et al.,* 1982). In particular, Montgomery

examined a section along 158W and noticed a trough at 12.5N, which, together with a ridge at 14N, marked "an unusually large disturbance within the North Equatorial Current." However, the trough and the ridge he found were more pronounced in the lower part of the pycnocline than at higher densities ($\sigma_\theta > 26.8$) below the pycnocline.

The thermostad (pycnostad) of the Equatorial 13°C Water is present between 4.5N and 4.5S with its center lying at 26.4–26.6 $\sigma_\theta$ (12.5–11°C; not 13°C at this longitude). It is bounded on the north by the subsurface North Equatorial Countercurrent associated with the sharp slope of the 26.6–27.0 $\sigma_\theta$ isopycnals and on the south by the subsurface South Equatorial Countercurrent associated with the slope of the 26.5–26.8 $\sigma_\theta$ isopycnals. Consistent with previous observations (e.g., Tsuchiya, 1981), it is best developed (thickest) 2–3° of latitude north and south of the equator with a local minimum thickness at the equator.

There is another slightly deeper thermostad (pycnostad) immediately north of the Equatorial 13°C Water. It is found from 4.5 to 13N at 9–10°C (26.7–26.8 $\sigma_\theta$) and contains the deeper portion of the subpycnocline high-salinity water described just above. This thermostad is invariably seen on earlier sections from the central and eastern Pacific (e.g., Tsubota, 1973; Craig *et al.,* 1981; Taft and Kovala, 1981; Taft *et al.,* 1982). A similar thermostad at about the same temperatures was reported between 6N and 15N along ~25W in the Atlantic (Tsuchiya *et al.,* 1992), but Wyrtki and Kilonsky (1984) appear to be the only previous investigators who noticed this thermostad in the equatorial Pacific. On the basis of the 1979–1980 Hawaii-Tahiti Shuttle Experiment data, they noted the presence of a large mass of homogeneous water at 9–11°C (depth 200–400 m) between 4N and 12N and suggested that it is a mixing product between "intermediate water masses" of the northern and southern hemispheres. They conjectured further that the main source of this water is to the east of their study area. However, the exact location and mechanism of formation remain obscure, although its low oxygen apparently precludes convective formation. No analogous thermostad exists south of the 13°C Water thermostad.

A few stations between 12S and 15S exhibit a weak vertical minimum of salinity at 26.6–26.7 $\sigma_\theta$ (not well defined in Fig. 3). This minimum is the South Pacific shallow salinity minimum (Reid, 1965, 1973a) analogous to the North Pacific shallow salinity minimum already described (Section 3b). It is distinct from the deeper minimum (~750 m), which is more clearly defined and is commonly referred to as the Antarctic Intermediate Water. The shallow salinity minimum originates in the Peru Current region off South America and is thought to extend first equatorward and then westward along the eastern and northern limbs of the subtropical anticyclonic gyre. It terminates at ~13S, 160W, about 2700 km west of the present section (Reid, 1973a, Fig. 1).

In about the same latitude range, centered at 12.5S, as the shallow salinity minimum, the isopycnals for 26.8–27.4 $\sigma_\theta$ show a trough flanked on both sides by

ridges. It is similar to the more pronounced trough observed near 12N and noted earlier in this section. This bowl-shaped isopycnal pattern is associated with a westward geostrophic flow in the northern half and an eastward flow in the southern half of the bowl relative to a deeper level (1500 dbar, for example). Lower-oxygen, higher-phosphate, higher-nitrate water is found in the northern half and higher-oxygen, lower-phosphate, lower-nitrate water is found in the southern half of the bowl (Figs. 5, 7 and 8; see also Figs. 11 and 12). In this density range oxygen is higher and nutrients are lower in the west than in the east of the equatorial South Pacific (Reid, 1965, 1986; Barkley, 1968; also Section 4), so that the oxygen and nutrient distributions are consistent with the geostrophic-flow directions indicated by the isopycnal slope. Although it is not obvious that this pattern is in any way related to the shallow salinity minimum, it suggests a complex circulation equatorward of the South Pacific subtropical gyre.

*d. South Pacific subtropical region.* The Subantarctic Mode Water (McCartney, 1977, 1982) is seen to extend as a well-developed pycnostad from the southern end of the section (33S) as far equatorward as 22S. The pycnostad is centered around 27.0 $\sigma_\theta$ at 33S and around a slightly higher density ( $\sim$ 27.05 $\sigma_\theta$) at its northern limit near 22S. It is wedged between the overlying primary pycnocline, which deepens equatorward, and the underlying secondary pycnocline, which shoals equatorward. The pycnostad coincides with a clearly defined vertical maximum of oxygen, but the oxygen maximum reaches farther north than the pycnostad. It lies below an oxygen minimum in the primary pycnocline and above the salinity minimum of the Antarctic Intermediate Water. The pycnostad is hardly recognizable as a thermostad in this latitude range (Fig. 2), although it manifests itself also as a thermostad (at 6–7°C) farther south (i.e., closer to the source region) on the Scorpio 43S section (Stommel *et al.*, 1973, Plate 1). Consistent with the present data, the Scorpio 28S section does not show a thermostad corresponding to the Subantarctic Mode Water pycnostad. The greater northward penetration of the pycnostad compared with the thermostad appears to be related to the existence of the salinity minimum (Antarctic Intermediate Water) at the base of the pycnostad. McCartney's (1982) sections of potential vorticity based on the Scorpio data illustrate that the Subantarctic Mode Water pycnostad has a density of 27.05 $\sigma_\theta$ at 95–105W along 43S and at 115–125W along 28S. These locations represent an approximate circulation path of the densest Mode Water we observed at 22S on our section.

## 4. Intermediate waters

In Figure 3 three distinct tongues of low-salinity water can be found at intermediate depths. Two of them extend from north to south, and the third one extends from south to north. The shallowest and least developed of the three is the salinity minimum of the North Pacific Intermediate Water and can be seen at 400–500 m

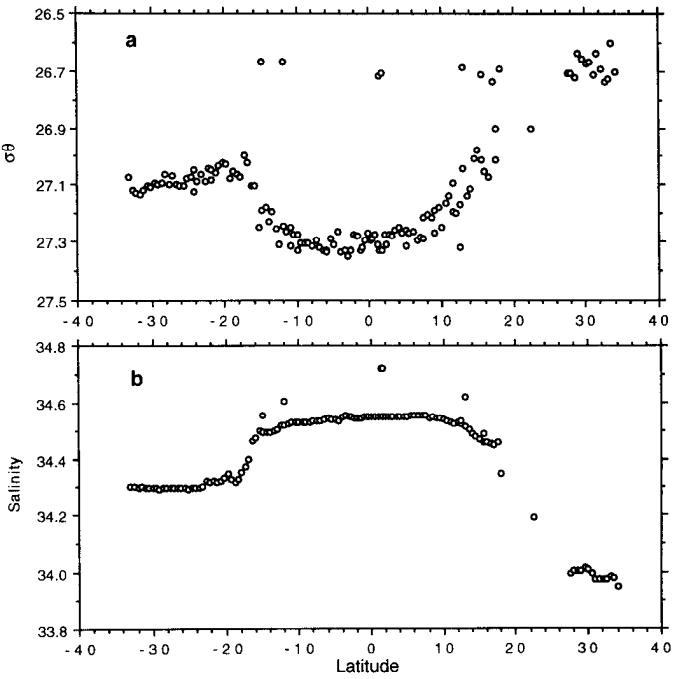


Figure 10. (a) Potential density $\sigma_\theta$ (kg m$^{-3}$) and (b) salinity at all salinity minima for $\sigma_\theta \geq 26.6$. The data are from bottle measurements along 135W.

from the northern end (34.5N) of the 135W section southward to 27N. Only parts of this tongue, including an isolated core at 28N, are depicted by the 34.0 isohalines in Figure 3, but it can be more clearly recognized as an isolated cluster of data points at 27–34N in Figure 10, which illustrates $\sigma_\theta$ and salinity at all salinity minima for $\sigma_\theta \geq 26.6$. This minimum has a core density of 26.6–26.7 $\sigma_\theta$ and can be distinguished from the less dense shallow salinity minimum (Section 3b). South of 27N, however, the North Pacific Intermediate Water is no longer recognized because the two salinity minima coalesce into a single layer of low salinity. The distribution of the North Pacific Intermediate Water, as defined as all salinity minima in the $\sigma_\theta$ range 26.6–27.0, has been mapped by Talley (1993) with use of a historical data set. Her map suggests that our 135W section just barely intersected its eastern edge, and its southern limit was located on our section several degrees of latitude farther south than on the map.

Another low-salinity tongue begins at about 500 m near 17N beneath the subpycnocline high-salinity water described in Section 3c. It extends southward to 6.5N with its core shifting to progressively greater depths. The core density ($\sigma_\theta$) increases sharply from 27.0 at 17N to 27.25 at 10N and then more slowly to 27.3 at 6.5N (Fig. 10a). Here it meets the third low-salinity tongue from the South Pacific (Antarctic Intermediate Water discussed next) resulting in a weak meridional

maximum of salinity. The minimum salinity increases from 34.45 at 17N to slightly above 34.55 at 6.5N. These low-salinity tongues and the meridional salinity maximum north of the equator are a common feature observed at almost all longitudes of the equatorial Pacific, as can be seen, for example, in the GEOSECS atlas (Craig *et al.*, 1981).

Yuan and Talley (1992) identified this low-salinity tongue south of 17N with the Antarctic Intermediate Water because its density is in the range of the Antarctic Intermediate Water to the south. In contrast, Wyrtki and Kilonsky (1982) interpreted a similar tongue observed in the central equatorial Pacific to be an equatorward extension of the "northern intermediate water" because the tongue stretches from north to south. However, it is much denser than the North Pacific Intermediate Water described just above, and there is no surface water in the open North Pacific as dense as this (e.g., Reid, 1965, 1973b), although weak ventilation does occur under sea-ice in the Okhotsk Sea (Kitani, 1973; Talley, 1991). Thus, Wyrtki and Kilonsky's "northern intermediate water" must have come from the South Pacific, although its low salinity requires that a considerable amount of the overlying fresher North Pacific water must also be incorporated into it by vertical mixing. Because of this complexity and the involvement of active vertical mixing, it is not possible to define a pair of North and South Pacific source waters, whose admixture with the overlying and underlying waters can account for the water characteristics of the low-salinity tongue in the density range of 27.0–27.3 $\sigma_\theta$. Without a clear definition of the source waters, any attempt to discuss the relative abundance of North and South Pacific waters in this low-salinity water does not seem to be of much significance. What is significant is that the water characteristics at the southern end of the tongue are those of the Antarctic Intermediate Water just to the south.

The third low-salinity tongue begins at 900 m at the southern end of the section and extends northward across the equator to 6.5N, where it reaches the meridional salinity maximum described just above. The low-salinity water in this tongue is collectively referred to as the Antarctic Intermediate Water, but our section shows two types of the Antarctic Intermediate Water, each characterized by meridionally uniform temperature, salinity, and density.

One is the subtropical type found between 33S and 17S, where the core density, temperature, and salinity are 27.05–27.1 $\sigma_\theta$, 5–6°C, and $\sim$34.3 (Fig. 10). The core depth is 900 m at 33S and decreases to 600 m at 17S. This northward rise of the low-salinity tongue is associated with a similar rise of isopycnals at intermediate depths, which in turn is associated with the westward-flowing limb of the subtropical gyre. The density ($\sigma_\theta$) at the core decreases only slightly from 27.1 to 27.05 between 33S and 17S. At 23–33S there is a thin and elongated low-salinity core centered at $\sim$25S and enclosed by the 34.3 isohaline. Two subsequent cruises, which extended the present section southward to Antarctica, confirm that this low-salinity water is separated from water of equally low salinity ($<$34.3) south of 50S. Oxygen and

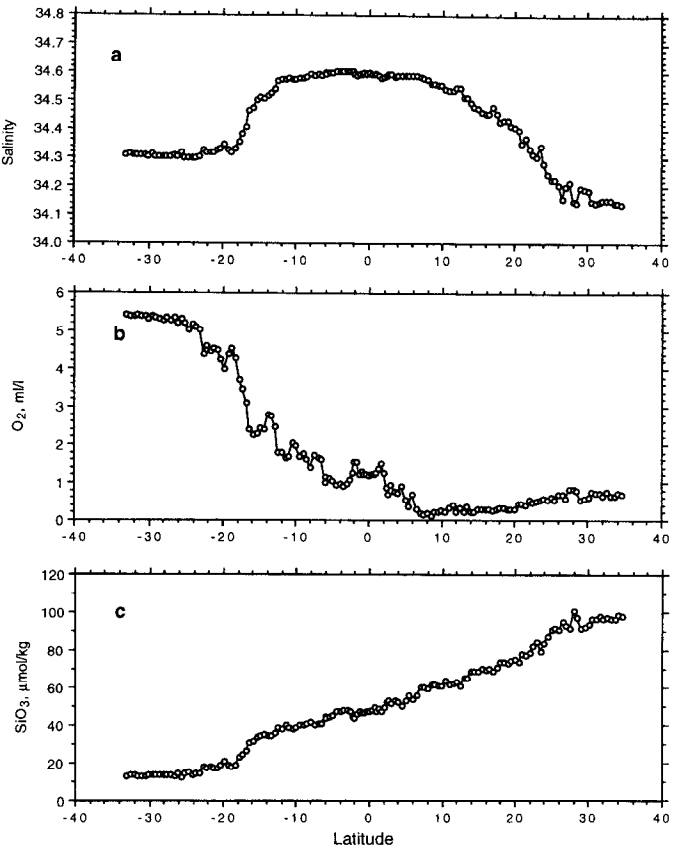


Figure 11. (a) Salinity, (b) oxygen (ml $l^{-1}$), and (c) silica (µmol $kg^{-1}$) at the 27.05 $\sigma_\theta$ isopycnal based on bottle measurements along 135W.

nutrients are also uniform near the southern end of the section, but oxygen begins to decrease and nutrients begin to increase from about 25S northward (Fig. 11). These water characteristics south of 17S represent the newest Antarctic Intermediate Water observed on our section. It enters the subtropical anticyclonic gyre in the eastern South Pacific and flows initially northward and then westward along the eastern and northern limbs of the gyre (Reid, 1965). At 135W its flow is predominantly westward.

Separated from the subtropical type by a transition zone at 17–10S, within which all characteristics show considerable meridional gradients, the other type of the Antarctic Intermediate Water is found at 800–900 m north of 10S (Fig. 10) and may be referred to as the equatorial type. It is notably uniform, both meridionally and vertically, in $\sigma_\theta$ ( ~ 27.3), temperature ( ~ 5°C), and salinity ( ~ 34.55). The meridional uniformity is seen to continue northward beyond the salinity maximum (at 6.5N) as far as 10N, well into the low-salinity tongue from the north. The vertical uniformity

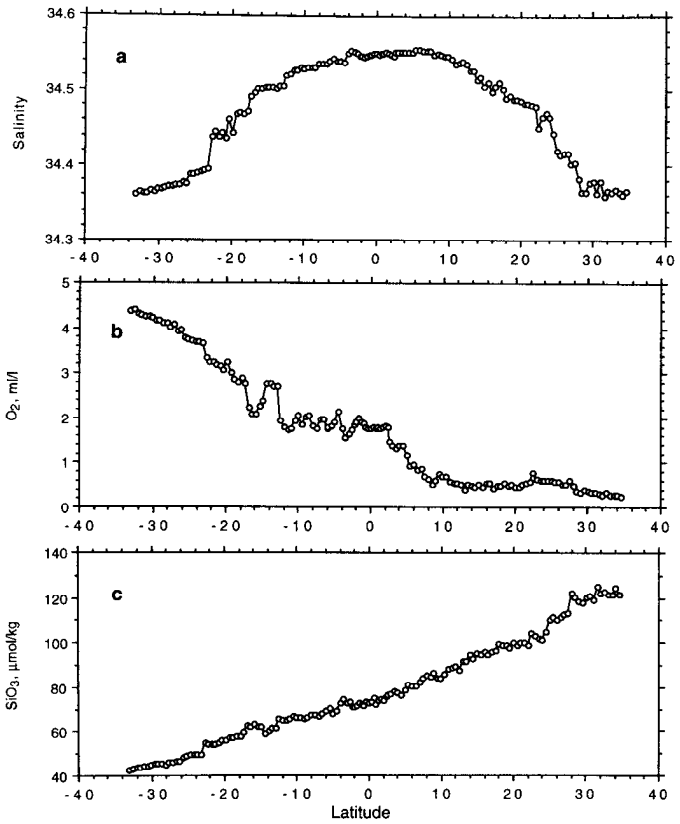


Figure 12. (a) Salinity, (b) oxygen (ml $l^{-1}$), and (c) silica (µmol $kg^{-1}$) at the 27.30 $\sigma_\theta$ isopycnal based on bottle measurements along 135W.

extends down to ~1100 m well below the salinity minimum as the rate of increase in salinity with depth below the minimum is smaller than that with height above it (Cochrane, 1958). In contrast to the uniformity in these conservative properties, nonconservative properties (oxygen and nutrients) exhibit significant basin-scale meridional gradients with high oxygen and low nutrients in the South Pacific and low oxygen and high nutrients in the North Pacific (Fig. 12). Superimposed on them are a number of smaller-scale variations, which are believed to reflect the zonal circulation pattern and discussed below.

While a discussion of how the Antarctic Intermediate Water spreads northward and how its characteristics are transformed from the subtropical to the equatorial type is beyond the scope of the present study based on a single section, some brief comments may be made here. The two types of the Antarctic Intermediate Water are associated with distinct circulation regimes. The subtropical type is confined in a single anticyclonic gyre, i.e., the South Pacific subtropical gyre, whereas the equato-

rial type occurs in a system of narrow alternating zonal flows in the region of the equator. The subtropical anticyclonic gyre and the equatorial zonal flows are connected by a northward-flowing western boundary undercurrent. Presumably, the Antarctic Intermediate Water is transmitted from the subtropical gyre to the equatorial region primarily by way of the western boundary undercurrent and then spreads from the western boundary into the interior of the equatorial region through the zonal flows (Reid, 1965; Reid and Mantyla, 1978). Because of this circulation pattern, oxygen is higher and nutrients are lower in the west than in the east of the equatorial region. Thus, at least some of the smaller-scale variations in oxygen and nutrients found within about 10° of the equator may be accounted for in terms of zonal flow (Fig. 12). This is an encouraging possibility, because it is difficult to estimate the geostrophic flow from the deep isopycnal slope in these low latitudes. Excluding those extrema that involve only one station, we find as many as seven meridional maxima and seven meridional minima of oxygen between 10N and 12S (Fig. 12b). Although some of these oxygen extrema are very weak and perhaps insignificant, it is possible that the maxima are associated with eastward flows and the minima are associated with westward flows. Nutrient extrema coincide generally well with the oxygen extrema (with maxima and minima reversed) providing consistent evidence. However, additional meridional sections with close station spacing are required to sort out zonally coherent permanent extrema from local disturbances.

The salinity increase (34.3 to 34.55) from the subtropical to the equatorial type indicates involvement of vertical mixing with the overlying warmer, saltier water and the underlying somewhat colder, saltier water. The density increase (27.05 to 27.3 $\sigma_\theta$) suggests that vertical mixing with the overlying water erodes the salinity minimum from the top shifting it to higher densities. In fact, relatively high-salinity water penetrates downward immediately above the salinity minimum within about 12° of the equator as recognized by the greater vertical separation (400 m) of the 34.6 isohaline from the bottom of the pycnocline (Fig. 3). The weak meridional maximum of salinity at ~6N also appears to be a result of vertical mixing. However, vertical mixing must take place primarily in the subtropical gyre and the western boundary current, because the Antarctic Intermediate Water's salinity and density at the east coast of Papua New Guinea have been increased to 34.50–34.53 and 27.26 $\sigma_\theta$ (Tsuchiya, 1991), which are already close to the values for the equatorial type observed at 135W.

## 5. Deep waters

The deep water in the Pacific originates from remote sources in the North Atlantic and Antarctic. As a result, the deep water below about 1500 m on this section is relatively featureless. Most properties increase or decrease slowly and monotonically with depth in most places. The only notable property extrema are a thick tongue of high silica centered at about 3000 m ($\sigma_4 \sim 45.8$) across the entire section, an oxygen

minimum ( $<3.6$ ml $l^{-1}$) at about 2000 m ($\sigma_2 \sim 36.9$) south of 25S, and phosphate and nitrate maxima that accompany the oxygen minimum.

The uniformity in potential temperature and salinity of the Pacific deep water was demonstrated by Cochrane (1958). His volumetric census of the Pacific Ocean water according to temperature-salinity characteristics indicates that the primary mode occurs at potential temperature 1.5°C, salinity 34.65 and that the modal water having characteristics between 1 and 2°C and between 34.6 and 34.7 amounts to 30% of the total volume of the Pacific Ocean. Together with the Indian Ocean deep water, which derives from the same North Atlantic sources and has similar uniform characteristics, the Pacific deep water forms the Common Water (Montgomery, 1958), the water type with the largest volume in the world ocean. This high degree of homogeneity of the Pacific deep water is clearly evident by comparing our sections with any full-depth sections from the Atlantic Ocean (e.g., Tsuchiya *et al.,* 1992, 1994).

The mid-depth vertical silica maximum in the Pacific is a well-documented feature. The water at this depth is derived from the south, but there are local sources of silica. Talley and Joyce (1992) assessed the relative importance of various possible sources and concluded that the silica maximum results primarily from dissolution of sinking particles. Their conclusion is consistent with the commonly accepted explanation that the silica maximum is maintained by a vertical balance between sinking particles and upwelling (e.g., Broecker and Peng, 1982) but contrasts with the argument of Edmond *et al.* (1979) that it is due to dissolution of bottom sediments. Recent observations indicate that hydrothermal venting, which ejects a considerable amount of silica, is more common than has been believed previously (J. E. Lupton, personal communication). This raises the possibility that Talley and Joyce (1992) might have underestimated the magnitude of the silica flux.

The high-silica tongue is fairly thick and vertically homogeneous as compared with the stronger vertical gradient above it. Therefore, it is difficult (and perhaps not important) to determine the exact depth of the silica maximum from our discrete water samples typically 200 m apart. On an average it lies at 3000 m and roughly coincides with the 45.8 $\sigma_4$ (36.98 $\sigma_2$) isopycnal (Fig. 13a). It is significantly deeper than the maximum observed farther north in the subarctic gyre (Talley *et al.,* 1991; Talley and Joyce, 1992). Between 20S and 23S, where the bottom is shallower than the maximum, the highest silica is naturally found at the bottom. The maximum silica concentration decreases southward almost linearly from 175 $\mu$mol $kg^{-1}$ at 34N to 130 $\mu$mol $kg^{-1}$ at 20S, but in the basin south of 23S it remains more uniform at 125–127 $\mu$mol $kg^{-1}$ (Fig. 13b). Between 2N and 12S the silica maximum is split into two maxima by a weak minimum. This feature is apparent in individual station data, but in Figure 6 it is only barely recognized by the peculiar shape of the 140 $\mu$mol $kg^{-1}$ isopleth near 9S. It can also be recognized in Figure 13a by vaguely defined two

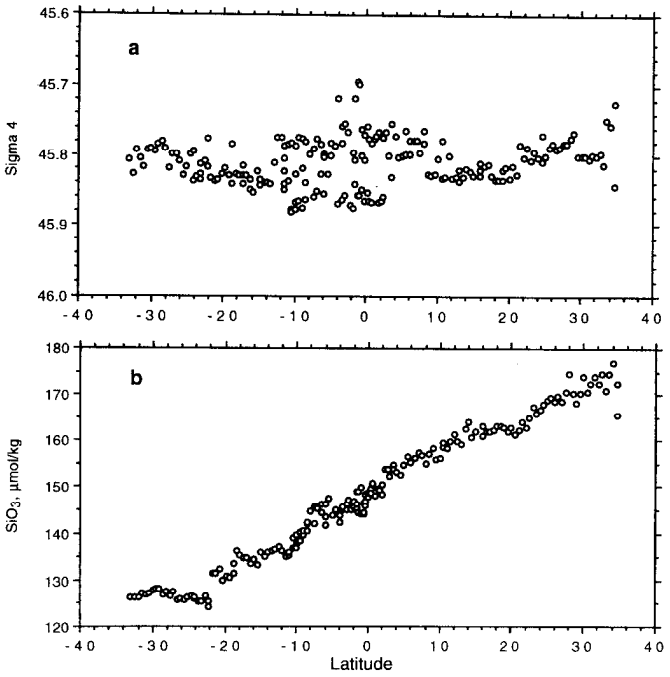


Figure 13. (a) Potential density $\sigma_4$ (kg $m^{-3}$) and (b) silica ($\mu$mol $kg^{-1}$) at the mid-depth silica maximum based on bottle measurements along 135W.

separate clusters of data points centered at 45.78 $\sigma_4$ and 45.85 $\sigma_4$ between 2N and 12S. The source of the low-silica water that separates the two maxima is not clear.

On the vertical section (Fig. 5), the vertical oxygen minimum south of 25S appears to be the southward continuation of the shallower, stronger minimum to the north, but examination of individual station data indicates that the two minima are separate. The shallower minimum peters out at Sta. 167 (27.1S), while the deeper minimum begins at Sta. 164 (25.7S) and extends all the way to the southern end of the section. It has been suggested that the deep oxygen minimum in the South Pacific is associated with the return flow of the deep and bottom waters that enter the North Pacific from the south (Reid, 1973c). The southward return flow is recognized as the low-oxygen water at 1500–2500 m east of the Tonga-Kermadec Ridge. Reid's (1986) maps of the adjusted steric height and isopycnal oxygen concentration in this depth range (his Figs. 36, 38, 43, and 45) can be taken to indicate that the southward return flow forms the western limb of an anticyclonic gyre developed between the Tonga-Kermadec Ridge and the East Pacific Rise and that the low-oxygen tongue observed south of 25S on our 135W section represents the return flow turning eastward and then northwestward along the anticyclonic gyre.

Although less obvious than the deep features described above, Talley and Johnson (1994) have noted that $\sigma_2$ isopycnals below 2000 m slope down from 20° toward 5–7°

on both sides of the equator and bulge upward at the equator (Fig. 4). Their isopycnal analysis of historical as well as recent high-quality, high-resolution data, including those from Tunes, indicates that this density structure is associated with westward-extending tongues of warm water centered at 5–8N and 10–15S and an eastward-extending tongue of cold water slightly south of the equator. The deep (2000–3000 m) westward flows north and south of the equator and eastward flow near the equator suggested by these tongues are consistent with previous observations of helium-isotope plumes discharged from the East Pacific Rise (Lupton and Craig, 1981; Ostlund *et al.,* 1987), but Talley and Johnson suggest that hydrothermal forcing is not likely the sole forcing mechanism for these deep flows, because of the existence of analogous features in the Atlantic Ocean.

## 6. Bottom waters

The cold, dense bottom water traveling eastward in the Antarctic Circumpoar Current protrudes northward into the Southwest Pacific Basin east of the New Zealand-Tonga-Kermadec ridges (Mantyla, 1975; Mantyla and Reid, 1983). Although this bottom flow is westward-intensified and our section lies in the east of the Basin, the region south of the bottom rise (near 23S) connecting the East Pacific Rise and the Tuamotu Archipelago is directly affected by it. The coldest, saltiest, densest, highest-oxygen, lowest-nutrient bottom water over the entire section is found here at the southern end of the section (Fig. 14). At the western boundary a slight vertical salinity maximum derived from the North Atlantic Deep Water is observed above the less saline bottom water (modified Antarctic Bottom Water; Taft *et al.,* 1991; Johnson *et al.,* 1994), but on our 135W section the salinity maximum occurs at the bottom, because the underlying less saline water is eradicated by vertical mixing. Thus, no bottom water in the strict sense (e.g., Pickard, 1964, p. 112) exists on our section. The term bottom water is used more loosely in the following to indicate the deepest water observed.

The cold, dense bottom water in the western boundary of the deep South Pacific flows northward through the Samoan Passage (Reid and Lonsdale, 1974; Taft *et al.,* 1991; Johnson *et al.,* 1994) and can be traced by its distinct characteristics into the Central Pacific Basin. Mantyla and Reid's (1983) maps (particularly that of oxygen) indicate that, after passing the Samoan Passage, part of it turns to the east along about 5S. This tongue of the dense, cold water implies an eastward flow south of the equator and is apparently the source of the local maxima of bottom density ($\sigma_4$) and oxygen and local minima of bottom temperature and nutrients which are well defined at ~5S in the basin between the Galapagos and Marquesas Fracture zones on the 135W section (Fig. 14).

The remaining part of the cold, dense bottom water continues northward across the equator and splits again into three branches. Of primary concern to us is the one that extends eastward into the Northeast Pacific Basin. It flows east through the

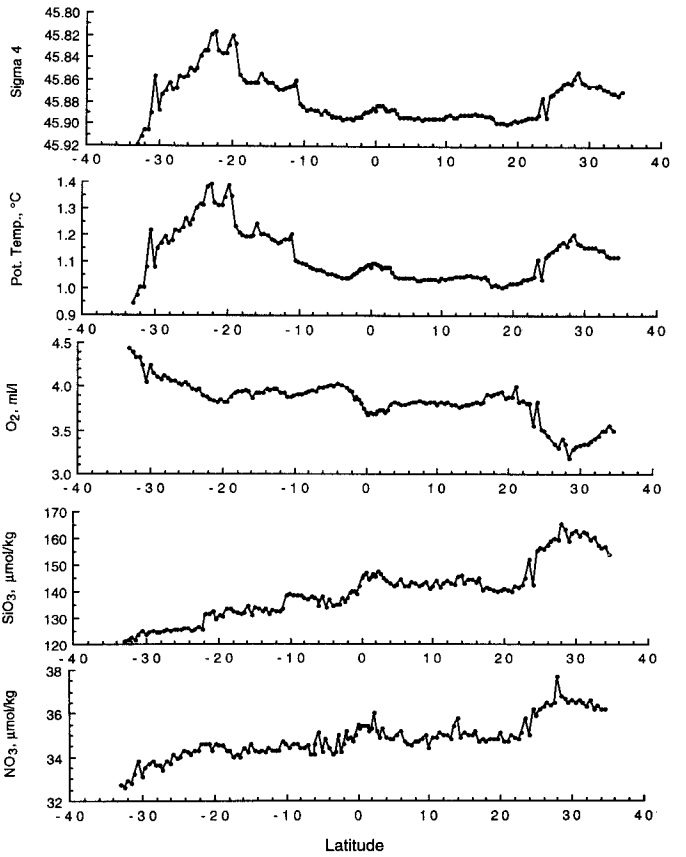


Figure 14. Properties at the deepest bottle along 135W. From top, potential density $\sigma_4$ (kg $m^{-3}$), potential temperature (°C), oxygen (ml $l^{-1}$), silica (µmol $kg^{-1}$), and nitrate (µmol $kg^{-1}$).

Horizon Passage (~19N, 169W) at the north end of the Line Islands Ridge (Edmond *et al.,* 1971) and the Clarion Passage (~12N, 165W) farther south at the west end of the Clarion Fracture Zone (Mantyla, 1975). The 135W section shows a rather broad local maximum of density (with concomitant extrema of the other properties) at 6–10 N (Fig. 14). This dense, cold bottom water can be taken to indicate that there is a band of eastward flow along the north side of the Clipperton Fracture Zone, as previous direct current-measurement data from this location suggested (Johnson, 1972). However, the bottom water in the Fracture Zone is blocked upstream by the Line Islands Ridge, so that the source of the eastward flow may be the bottom water from the Clarion Passage that has turned to the south along the eastern flank of the Line Islands Ridge.

With use of limited data that were available, Wong (1972) examined near-bottom water characteristics at four longitudes between 130W and 170W in the equatorial

Pacific and noticed marginally colder, higher-oxygen, lower-silica bottom waters centered at about 10N and 5S. He postulated that these waters are associated with eastward zonal flows and identified their possible sources. Our findings from the 135W section described just above largely support his inferences.

Another local maximum of bottom $\sigma_4$ occurs on our section at ~18N in the deep basin bounded on the south by the Clarion Fracture Zone (Fig. 14). This represents the densest (~45.90 $\sigma_4$), coldest (~1.00°C) bottom water we observed north of the equator and is most likely to derive from the Clarion Passage. It appears to indicate the principal pathway of the bottom water in the Northeast Pacific Basin.

There is relatively dense bottom water near 34N in the deep basin between Murray and Pioneer Fracture zones (Fig. 14). Its source is not certain, but it may come from the eastward flow through the Horizon Passage, which turns northward around the southeast corner of the Hawaiian Ridge (Edmond *et al.,* 1971).

These local maxima of the bottom density are (necessarily) accompanied by local minima, which occur at the equator, ~14N, and ~28N (Fig. 14). Although the bottom rises to significantly lesser depths at the equator and near 28N, this shoaling alone does not account for the lower densities observed over the bottom rises. As can be seen in the vertical section (Fig. 4), near-bottom isopycnals deepen toward each rise on both sides of it (a similar but more pronounced isopycnal pattern is also seen at the crest of the ridge near 23S). Thus, the local minima of $\sigma_4$ (and accompanying extrema of the other properties) appear to be related to the flow pattern, which may involve westward zonal flows of the less dense, warmer, fresher, lower-oxygen, higher-nutrient bottom water from the eastern boundary region of the North Pacific (Mantyla and Reid, 1983, Fig. 2).

## 7. Conclusion

In the preceding sections various features of the water-property distributions observed along the new section at 34N/135W have been described. Some of these features are summarized below.

(1) The subarctic (34N), northern subtropical (33N), and subtropical (31N) fronts were clearly defined in the surface-layer salinity field. The first two fronts lay so close together that they would not have been differentiated without the high horizontal resolution of the present data.

(2) The highest surface temperature (~29°C) was observed at 7N within the salinity front that marked the southern boundary of the equatorial low-salinity surface water associated with high precipitation. The surface temperature in this region was found to be nearly 1.5°C higher than the long-term monthly mean for June, and the well-known temperature minimum due to upwelling at the equator was only weakly recognized. This positive temperature anomaly subsequently developed into an ocean-wide El Niño condition.

(3) Relatively high-salinity water, which contained a vertical maximum of salinity

at 26.5–26.7 $\sigma_\theta$ and was overlain by the equatorial low-salinity surface water, dominated the subpycnocline layer between the equator and 17N. Its immediate source water is found between 115W and the coast of Central America and appears to come from the south across the equator.

(4) The subpycnocline isopycnals for 26.8–27.5 $\sigma_\theta$ exhibited a well-defined trough at 12N. Previous data indicate that this trough has been frequently observed at about the same latitude in the central and eastern Pacific and is presumed to be a semi-permanent feature. A similar trough of essentially the same isopycnals was observed also at 12.5S. The property distributions along the isopycnals show no clear signal of the northern trough (Figs. 10 and 11) and suggest that it is associated with local recirculation. In contrast, there are clear changes in the isopycnal oxygen, phosphate, and nitrate concentrations across the southern trough apparently reflecting the zonal flow pattern.

(5) A permanent thermostad (pycnostad) at 9–10°C (26.7–26.8 $\sigma_\theta$) was observed between 4.5N and 15N. It lay just north of the pycnostad of the Equatorial 13°C Water but was slightly deeper. Although previous data indicate that this thermostad is a permanent feature in the central and eastern Pacific, the location and mechanism of its formation remain obscure.

(6) The pycnostad of the Subantarctic Mode Water (centered at 27.0–27.05 $\sigma_\theta$) was well developed from the southern end of the section (33S) to 22S, but was hardly recognized as a thermostad. The pycnostad coincided with an oxygen maximum, and at the bottom of the pycnostad lay the salinity minimum associated with the Antarctic Intermediate Water (subtropical type described in (8) below). On the basis of the Scorpio and other data, the pathway of the densest Mode Water (27.05 $\sigma_\theta$) observed at 22S on our section can be traced back to 28S, 120W, farther to 43S, 100W, and ultimately to its outcrop region near 53S, 90W just west of the southern tip of the South American Continent.

(7) The North Pacific Intermediate Water, characterized by a salinity minimum at 26.6–26.7 $\sigma_\theta$, was present on this section only to the north of 27N, as was already shown by Yuan and Talley (1992).

(8) The salinity minimum of the Antarctic Intermediate Water extended as a prominent low-salinity tongue from the southern end of the section northward across the equator to 6.5N, where it was met by another low-salinity tongue from the north resulting in a weak meridional maximum of salinity. The southern tongue contained two types of the Antarctic Intermediate Water, each characterized by meridionally uniform temperature, salinity, and density. One type was found south of 17S in the subtropical anticyclonic gyre and had the core characteristics of 5–6°C, 34.3, and 27.05–27.1 $\sigma_\theta$. The other type was observed north of 10S within the region of the equatorial zonal currents and showed the core characteristics of 5°C, 34.55, and 27.3 $\sigma_\theta$. The latter type was found to be especially uniform both vertically and meridionally; the characteristics of the Antarctic Intermediate Water of the equato-

rial type extended northward beyond the meridional maximum of salinity (at 6.5N) as far as 10N, well into the low-salinity tongue from the north.

(9) The deep water below about 1500 m was found to be relatively featureless in terms of the property distributions, since the major part of it originates from remote sources in the North Atlantic. Most properties showed a monotonic increase or decrease with depth in most places. The only property extrema we observed are a thick high-silica tongue centered at about 3000 m (45.8 $\sigma_4$) and extending southward across the entire section, an oxygen minimum at about 2000 m (36.9 $\sigma_2$) south of 25S, and phosphate and nitrate maxima that accompany the oxygen minimum. Despite this apparent lack of features, it was recognized that $\sigma_2$ isopycnals below 2000 m sloped down from 20° toward 5–7° on both sides of the equator and bulged upward at the equator. Talley and Johnson's (1994) isopycnal analysis of the present data, combined with high-quality historical and other WHP data, clearly showed that this density structure is associated with deep (2000–3000 m) westward flows at 5–8N and 10–15S and an eastward flow at 1–2S.

(10) The coldest, saltiest, densest, highest-oxygen, lowest-nutrient bottom water over the entire section was found at its southern end. It is a direct influence of the cold, dense bottom water that flows into the Southwest Pacific Basin from the Antarctic Circumpolar Current along the eastern flank of the New Zealand-Tonga-Kermadec ridges.

(11) Local maxima of bottom density ($\sigma_4$) and oxygen, coincident with local minima of bottom temperature and nutrients, were observed at 5S, 6–10N, 18N, and 34N. These locations are evidently determined by the bottom topography characterized by numerous fracture zones oriented east-west and represent the pathways of eastward flows into the Northeast Pacific Basin of the cold, dense bottom water that separates from the northward-flowing western boundary undercurrent. Between these local property extrema were (necessarily) found opposite extrema, which were located at the equator, 14N, and 28N. These opposite extrema may be associated with westward zonal flows of the less dense, warmer, fresher, lower-oxygen, higher-nutrient bottom water from the eastern boundary region of the North Pacific.

It is clear from this work that high-quality, high-resolution CTD/hydrographic data such as those presented here add much to our understanding of the large-scale ocean circulation. They reveal not only additional details of previously known features but numerous new features that have not been observed before. More comprehensive and thorough analyses of combined data, including those of chemical tracers, from this and other WHP sections are eagerly awaited.

*Acknowledgments.* This study was supported by the WOCE Hydrographic Program funded by the National Science Foundation through Grants OCE89-18961 and OCE90-04394. We would like to thank J. H. Swift and R. G. Peterson for serving as chief and co-chief scientists on Tunes Leg 2. The field work was made possible by the dedicated support provided by the

Oceanographic Data Facility at Scripps Institution of Oceanography and the captain and crew of R/V *Thomas Washington.*

## REFERENCES

Barkley, R. A. 1968. Oceanographic atlas of the Pacific Ocean. University of Hawaii Press, Honolulu, 20 pp + 156 figures.

Broecker, W. S. and T.-H. Peng. 1982. Tracers in the Sea. Lamont-Doherty Geological Observatory, Palisades, 690 pp.

Cannon, G. A. 1966. Tropical waters in the western Pacific Ocean, August–September 1957. Deep-Sea Res., *13,* 1139–1148.

Cochrane, J. D. 1958. The frequency distribution of water characteristics in the Pacific Ocean. Deep-Sea Res., *5,* 111–127.

Craig, H., W. S. Broecker and D. Spencer. 1981. GEOSECS Pacific Expedition, Vol. 4, Sections and profiles. National Science Foundation, Washington, D. C., 251 pp.

Edmond, J. M., Y. Chung and J. G. Sclater. 1971. Pacific bottom water: penetration east around Hawaii. J. Geophys. Res., *76,* 8089–8097.

Edmond, J. M., S. S. Jacobs, A. L. Gordon, A. W. Mantyla and R. F. Weiss. 1979. Water column anomalies in dissolved silica over opaline pelagic sediments and the origin of the deep silica maximum. J. Geophys. Res., *84,* 7809–7826.

Hires, R. I. and R. B. Montgomery. 1972. Navifacial temperature and salinity along the track from Samoa to Hawaii, 1957–1965. J. Mar. Res., *30,* 177–200.

Johnson, D. A. 1972. Eastward-flowing bottom currents along the Clipperton Fracture Zone. Deep-Sea Res., *19,* 253–257.

Johnson, G. C., D. L. Rudnick and B. A. Taft. 1994. Bottom water variability in the Samoa Passage. J. Mar. Res., *52,* 177–196.

Kitani, K. 1973. An oceanographic study of the Okhotsk Sea—particularly in regard to cold waters. Bull. Far Seas Fish. Res. Lab., *9,* 45–77.

Levitus, S. 1982. Climatological atlas of the world ocean. NOAA Prof. Pap, *13,* 173 pp.

Lupton, J. E. and H. Craig. 1981. A major helium-3 source at 15°S on the East Pacific Rise. Science, *214,* 13–18.

Lynn, R. J. 1964. Meridional distribution of temperature-salinity characteristics of Pacific Ocean surface water. J. Mar. Res., *22,* 70–82.

—— 1986. The subarctic and northern subtropical fronts in the eastern North Pacific Ocean in spring. J. Phys. Oceanogr., *16,* 209–222.

Mantyla, A. W. 1975. On the potential temperature in the abyssal Pacific Ocean. J. Mar. Res., *33,* 341–354.

Mantyla, A. W. and J. L. Reid. 1983. Abyssal characteristics of the World Ocean waters. Deep-Sea Res., *30,* 805–833.

McCartney, M. S. 1977. Subantarctic Mode Water, *in* A Voyage of Discovery, George Deacon 70th Anniversary Volume, M. Angel, ed., Pergamon Press, Oxford, 103–119.

—— 1982. The subtropical recirculation of Mode Waters. J. Mar. Res., *40*(Suppl.), 427–464.

Montgomery, R. B. 1954. Analysis of a Hugh M. Smith oceanographic section from Honolulu southward across the equator. J. Mar. Res., *13,* 67–75.

—— 1958. Water characteristics of Atlantic Ocean and of world ocean. Deep-Sea Res., *5,* 134–148.

Montgomery, R. B. and E. D. Stroup. 1962. Equatorial waters and currents at 150°W in July–August 1952. Johns Hopkins Oceanogr. Stud., *1,* 68 pp.

Ostlund, G., H. Craig, W. S. Broecker and D. Spencer. 1987. GEOSECS Atlantic, Pacific, and Indian Ocean Expeditions, Vol. 7, Shorebased data and graphics. National Science Foundation, Washington, D. C., 200 pp.

Pickard, G. L. 1964. Descriptive Physical Oceanography: An introduction. The MacMillan Company, New York, 199 pp.

Puls, C. 1895. Oberflächen Temperaturen und Strömungsverhältnisse des Aequatorialgürtels des Stillen Ozeans. Arch. Deutsch. Seewarte, *18*(1), 38 pp.

Reid, J. L., Jr. 1965. Intermediate Waters of the Pacific Ocean. Johns Hopkins Oceanogr. Stud., *2,* 85 pp.

—— 1973a. The shallow salinity minima of the Pacific Ocean. Deep-Sea Res., *20,* 51–68.

—— 1973b. Northwest Pacific OceanWaters in Winter. Johns Hopkins Oceanogr. Stud., *5,* 96 pp.

—— 1973c. Transpacific hydrographic sections at Lats. 43°S and 28°S: the SCORPIO Expedition—III. Upper water and a note on southward flow at mid-depth. Deep-Sea Res., *20,* 39–49.

—— 1986. On the total geostrophic circulation of the South Pacific Ocean: flow patterns, tracers and transports. Prog. Oceanogr., *16,* 1–61.

Reid, J. L. and P. F. Lonsdale. 1974. On the flow of water through the Samoan Passage. J. Phys. Oceanogr., *4,* 58–73.

Reid, J. L. and A. W. Mantyla. 1978. On the mid-depth circulation of the North Pacific Ocean. J. Phys. Oceanogr., *8,* 946–951.

Robinson, M. K. 1976. Atlas of North Pacific Ocean monthly mean temperatures and mean salinities of the surface layer. Naval Oceanographic Office Reference Publication 2, Washington, D. C., 19 pp + 173 figures.

Roden, G. I. 1980. On the subtropical frontal zone north of Hawaii during winter. J. Phys. Oceanogr., *10,* 342–362.

Stommel, H., E. D. Stroup, J. L. Reid and B. A. Warren. 1973. The transpacific hydrographic sections at Lats. 43°S and 28°S: the SCORPIO Expedition—I. Preface. Deep-Sea Res., *20,* 1–7.

Taft, B. A., A. Cantos-Figuerola and P. Kovala. 1982a. Vertical sections of temperature, salinity, thermosteric anomaly and zonal geostrophic velocity from NORPAX Shuttle Experiment. Part 3. NOAA Data Repor ERL PMEL-7, 89 pp.

Taft, B. A., S. P. Hayes, G. E. Friederich and L. A. Codispoti. 1991. Flow of abyssal water into the Samoa Passage. Deep-Sea Res., *38*(Suppl. 1), S103–S128.

Taft, B. A. and P. Kovala. 1981. Vertical sections of temperature, salinity, thermosteric anomaly and zonal geostrophic velocity from NORPAX Shuttle Experiment. Part 1. NOAA Data Report ERL PMEL-3, 98 pp.

Taft, B. A., P. Kovala and A. Cantos-Figuerola. 1982b. Vertical sections of temperature, salinity, thermosteric anomaly and zonal geostrophic velocity from NORPAX Shuttle Experiment. Part 2. NOAA Data Report ERL PMEL-5, 94 pp.

Talley, L. D. 1991. An Okhotsk Sea water anomaly: implications for ventilation in the North Pacific. Deep-Sea Res., *38*(Suppl. 1), S171–S190.

—— 1993. Distribution and formation of North Pacific Intermediate Water. J. Phys. Oceanogr., *23,* 517–537.

Talley, L. D. and G. C. Johnson. 1994. Deep, zonal subequatorial currents. Science, *263,* 1125–1128.

Talley, L. D. and T. M. Joyce. 1992. The double silica maximum in the North Pacific. J. Geophys. Res., *97,* 5465–5480.

Talley, L. D., T. M. Joyce and R. A. DeSzoeke. 1991. Transpacific sections at 47°N and 152°W: Distribution of properties. Deep-Sea Res., *38*(Suppl. 1), S63–S82.

Tsubota, H. 1973. Preliminary report of the Hakuho Maru cruise KH-71-5 (Phoenix Expedition). Ocean Res. Inst., University of Tokyo.

Tsuchiya, M. 1968. Upper waters of the intertropical Pacific Ocean. Johns Hopkins Oceanogr. Stud., *4,* 50 pp.

—— 1975. Subsurface countercurrents in the eastern equatorial Pacific Ocean. J. Mar. Res., *33*(Suppl.), 145–175.

—— 1981. The origin of the Pacific Equatorial 13°C Water. J. Phys. Oceanogr., *11,* 794–812.

—— 1991. Flow path of the Antarctic Intermediate Water in the western equatorial South Pacific Ocean. Deep-Sea Res., *38*(Suppl. 1), S273–S279.

Tsuchiya, M., L. D. Talley and M. S. McCartney. 1992. An eastern Atlantic section from Iceland southward across the equator. Deep-Sea Res., *39,* 1885–1917.

—— 1994. Water-mass distributions in the western South Atlantic; a section from South Georgia Island (54S) northward across the equator. J. Mar. Res., *52,* 55–81.

U. S. WOCE Office. 1989. U. S. WOCE Implementation Plan. U. S. WOCE Implementation Report No. 1, College Station, Texas, 134 pp.

Wong, C. S. 1972. Deep zonal water masses in the equatorial Pacific Ocean inferred from anomalous oceanographic properties. J. Geophys. Res., *77,* 7196–7202.

Wyrtki, K. and B. Kilonsky. 1982. Transequatorial water structure during the Hawaii to Tahiti Shuttle Experiment. Hawaii Institute of Geophysics, University of Hawaii, HG-82-5, 65 pp.

—— 1984. Mean water and current structure during the Hawaii-to-Tahiti Shuttle Experiment. J. Phys. Oceanogr., *14,* 242–254.

Yoshida, K. 1955. Coastal upwelling off the California coast. Rec. Oceanogr. Works Jap., *2*(2), 8–20.

Yoshida, K. and M. Tsuchiya. 1957. Northward flow in lower layers as an indicator of coastal upwelling. Rec. Oceanogr. Works Jap., *4*(1), 14–22.

Yuan, X. and L. D. Talley. 1992. Shallow salinity minima in the North Pacific. J. Phys. Oceanogr., *22,* 1302–1316.

Received: *13 July 1995;* revised: *2 November, 1995.*